

Lawrence Berkeley National Laboratory

Advanced Light Source

Title

Probing the role of the barrier layer in magnetic tunnel junction transport

Permalink

<https://escholarship.org/uc/item/35b9k5xf>

Journal

Physical Review B, 76(22)

ISSN

2469-9950

Authors

Nelson-Cheeseman, BB
Chopdekar, RV
Alldredge, LMB
[et al.](#)

Publication Date

2007-12-01

DOI

10.1103/physrevb.76.220410

Peer reviewed

Probing the role of the barrier layer in magnetic tunnel junction transport

B. B. Nelson-Cheeseman,^{1,*} R. V. Chopdekar,^{2,1} L. M. B. Alldredge,^{2,1} J. S. Bettinger,¹ E. Arenholz,³ and Y. Suzuki¹

¹*Department of Materials Science and Engineering,
University of California, Berkeley, California 94720, USA*

²*School of Applied and Engineering Physics,
Cornell University, Ithaca, New York 14853, USA*

³*Advanced Light Source, Lawrence Berkeley National
Laboratory, Berkeley, California 94720, USA*

Abstract

Magnetic tunnel junctions with a ferrimagnetic barrier layer have been studied to understand the role of the barrier layer in the tunneling process - a factor that has been largely overlooked until recently. Epitaxial oxide junctions of highly spin polarized $\text{La}_{0.7}\text{Sr}_{0.3}\text{MnO}_3$ and Fe_3O_4 electrodes with magnetic NiMn_2O_4 (NMO) insulating barrier layers provide a magnetic tunnel junction system in which we can probe the effect of the barrier by comparing junction behavior above and below the Curie temperature of the barrier layer. When the barrier is paramagnetic, the spin polarized transport is dominated by interface scattering and surface spin waves; however, when the barrier is ferrimagnetic, spin flip scattering due to spin waves within the NMO barrier dominates the transport.

PACS numbers: 75.47.-m, 85.75.-d, 72.25.Mk, 75.70.Cn

The magnetic tunnel junction (MTJ) is one of the most simple spin polarized devices whose transport behavior has yet to be completely understood. Its basic device characteristics have been explained in terms of a simple quantum mechanical model of two spin polarized reservoirs separated by a potential barrier over two decades ago.¹ In this picture, depending on the relative orientation of the magnetization in the two ferromagnetic electrodes, a high or low resistance results. However, this simplified picture does not accurately describe the behavior of real MTJs. Improvements in the electrode-barrier interfaces have now led to the observation of magnetic tunnel junction behavior at room temperature² and the realization that the transport through these structures is extremely sensitive to the interface scattering and spin polarized interface density of states of the electrodes.³ It was not until recently, however, that the importance of understanding the role of the barrier layer in the tunneling process was recognized in experimental and theoretical studies of MTJs with MgO barriers.⁴ In these junctions, a number of factors dictated by the barrier layer were recognized to be important, including the chemical bonding between the atoms at the electrode-barrier interface, interface resonance states, and the symmetries of the propagating states in the electrodes and evanescent states in the barrier layer. In order to develop a complete picture of spin polarized transport in MTJs, the role of the barrier layer in the tunneling process as well as electrode-barrier interface effects must be generalized.

There have been some efforts to elucidate the role of the barrier layer by introducing magnetism into the barrier through dilute doping of a nonmagnetic barrier with magnetic ions or the use of paramagnetic barriers. Jansen *et al.* found that δ -doping of Al₂O₃ barriers with Fe ions increased the junction magnetoresistance (JMR) as a function of Fe content in the barrier.⁵ The enhanced JMR was explained in terms of spin filtering of the tunneling electrons, whereby a preferential transmission (increased conductance) exists for one type of spin due to the polarized barrier states.⁶ Other studies of MTJs with paramagnetic barriers suggest that the presence of paramagnetism in the barrier layer does not preclude large JMR values or distinct switching characteristics.^{7,8,9} These results suggest that magnetism in the barrier can be spin preserving rather than adding to spin-flip scattering via spin waves. If weak magnetism in the barrier is spin preserving, then incorporating long-range ferromagnetic order in the barrier layer of a MTJ should provide a system where the role of the barrier layer can be readily probed as long as the barrier does not magnetically couple the two ferromagnetic electrodes.

In this paper, we demonstrate magnetic tunnel junction behavior in junctions with ferromagnetic electrodes and a barrier layer with long range ferrimagnetic order. Comparison of junction behavior when the barrier layer is ferrimagnetic to when it is paramagnetic enables us to probe the role of the barrier layer in one of the simplest spin polarized devices. In particular, we focus on $\text{Fe}_3\text{O}_4/\text{NiMn}_2\text{O}_4(\text{NMO})/\text{LSMO}$ (spinel/spinel/perovskite) junctions to preserve the magnetic decoupling of the electrodes in the presence of a magnetic barrier layer. Magnetization measurements of the layers as well as at the interfaces indicate that we have two ferromagnetic electrodes that switch independently despite the presence of a ferrimagnetic-paramagnetic barrier layer. Spin polarized transport measurements reveal junction magnetoresistance values as high as -30% (normalized to 8 kOe). Two different conduction mechanisms are observed which directly highlight the passive or active role of the barrier layer in the spin transport. Above the T_C of the NMO barrier, when the barrier layer is paramagnetic, the electrode-barrier interfaces dominate the spin transport, resulting in an asymmetric bias dependence of the JMR and inelastic tunneling spectra (IETS). Below the T_C of the NMO barrier, the ferrimagnetism in the barrier dominates the spin transport, resulting in a transition to a symmetric bias dependence of the JMR and IETS.

The trilayers of $\text{Fe}_3\text{O}_4/\text{NMO}/\text{LSMO}$ were grown by pulsed laser deposition on SrTiO_3 (STO) (110) substrates following Ref. 9. LSMO and Fe_3O_4 were chosen for their highly spin polarized nature as both have been theorized and shown to be half-metallic.⁸ Since isostructural barrier layers have been shown to greatly increase the JMR values for epitaxial Fe_3O_4 MTJs,⁸ a ferrimagnetic spinel, NiMn_2O_4 , was selected. NMO films were grown at 550 °C in 10 mTorr of a 99% $\text{N}_2/1\%$ O_2 gaseous mixture. For these deposition conditions, the NMO film was insulating with an onset of ferrimagnetism around 60 K, a large coercive field of 1.6 T at 30 K, a magnetization of $0.8 \mu_B$ per formula unit, and an inverse spinel cation site distribution.¹⁰ Barrier thicknesses were 20, 30, and 45 Å. The films grow epitaxially on the STO substrate with excellent crystallinity as confirmed by x-ray diffraction and Rutherford backscattering channeling measurements. The MTJs were fabricated by conventional lithography and Ar ion milling.

The bulk magnetism of the samples was investigated by a superconducting quantum interference device (SQUID) magnetometer, while the interface magnetization was investigated by X-ray magnetic circular dichroism (XMCD) at the Advanced Light Source on BL4.0.2. The transport measurements were conducted in magnetic fields up to 8kOe and

temperatures from 15 to 300 K. The bias and temperature dependence of the JMR were calculated in accordance with Julliere's model by the following equation: $\frac{\Delta R}{R(P)} \times 100$, where $\Delta R = R_{AP} - R_P$,¹ and the reference (parallel magnetization) resistance was taken at 8 kOe.

Magnetic hysteresis loops of the trilayers show distinct switching of the two ferromagnetic layers. We observe large coercive field differences between the LSMO and Fe₃O₄, thus creating well-defined parallel and antiparallel magnetization states at all temperatures. However, the magnetization of the NMO barrier cannot be probed with bulk methods due to its small magnetic signal compared to that of the ferromagnetic electrodes.

In order to probe the magnetic behavior at the interfaces and within the barrier layer, element-specific XMCD was used in the total electron yield mode. Since the total electron yield method is surface sensitive, we studied heterostructures of LSMO (40 nm)/NMO (5 nm) and LSMO (40 nm)/NMO (5 nm)/Fe₃O₄ (5 nm) to probe both interfaces. Figure 1 shows the Mn XMCD spectra for the LSMO/NMO bilayer sample for various temperatures. A pronounced valley (peak) in the XMCD is evident at 640 eV (642.5 eV) at lower temperatures resembling XMCD spectra of NMO single films.¹⁰ This feature disappears above 60 K, resulting in Mn XMCD spectra at 80 and 100 K resembling that of LSMO thin films.¹¹ In order to probe the origins of the Mn magnetism, hysteresis loops were taken at 640 and 642.5 eV. Hysteresis loops taken at 642.5 eV show magnetically soft Mn with coercive fields <0.5 kOe over the entire temperature range. Those taken at 640 eV show a transition from the soft loops above 60 K (similar to those at 642.5 eV) to magnetically harder loops that do not reach saturation by 8 kOe, resembling SQUID hysteresis loops of single NMO films. This transition indicates the onset of ferrimagnetism in the magnetically hard NMO barrier at 60 K.

From the XMCD hysteresis loops in Fig. 1, it is clear that the Mn magnetism in the NMO and LSMO is probed at 640 eV whereas only the LSMO magnetism is probed at 642.5 eV. The observation of soft hysteresis loops at all temperatures for Mn at 642.5 eV is direct evidence that the LSMO is not exchange coupled to the magnetically harder NMO whose onset of ferrimagnetism is verified at 640 eV. A comparison of the hysteresis loops taken at 640 and 642.5 eV at 55 K is further evidence that only a mere superposition of the Mn signals from the LSMO and NMO takes place, and not a correlated magnetic coupling effect. The lack of magnetic coupling at the LSMO-NMO interface likely arises from misfit dislocations due to the lattice mismatch between the perovskite and spinel structures, providing for easy

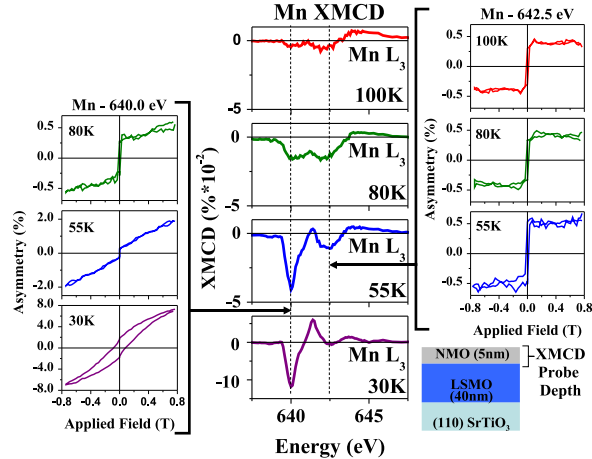


FIG. 1: (Color online) Surface sensitive XMCD investigating the LSMO-NMO interface magnetism. Normalized Mn XMCD of the NMO-LSMO interface, and Mn hysteresis loops taken at 640.0 eV and 642.5 eV as a function of temperature.

180° domain wall creation at the LSMO-NMO interface, and decoupling the magnetic layers. This lack of coupling at this interface enables the independent switching of the two electrodes below the magnetic ordering temperature of the NMO. This independent switching is further verified in symmetric minor loops of LSMO.

XMCD hysteresis loops were also taken at various temperatures on the trilayer sample to probe the magnetic behavior of the NMO-Fe₃O₄ interface. A distinct increase in coercive field of the Fe₃O₄ layer is seen below the NMO T_C . This increase, as well as coincident Fe, Mn, and Ni loops, reveals the presence of strong ferromagnetic coupling between the two spinel layers, while still maintaining the onset of NMO ferrimagnetism.¹²

Now that we have established the magnetic decoupling of the ferromagnetic electrodes despite the magnetic barrier, we focus on the spin transport in the junction above and below the T_C of the barrier layer. As shown in Fig. 2(a), transitions in the magnetization hysteresis loops coincide well with large and abrupt transitions in the JMR. The antiparallel LSMO-Fe₃O₄ magnetization configuration is the low resistance state, resulting in a negative magnetoresistance. This is due to the opposite spin polarizations of LSMO and Fe₃O₄ electrodes, which are majority and minority spin polarized, respectively.⁸

The temperature dependence of the JMR is studied to investigate the effect of the barrier layer magnetism on the magnetotransport of the junctions [Fig. 2(b)]. The maximum JMR

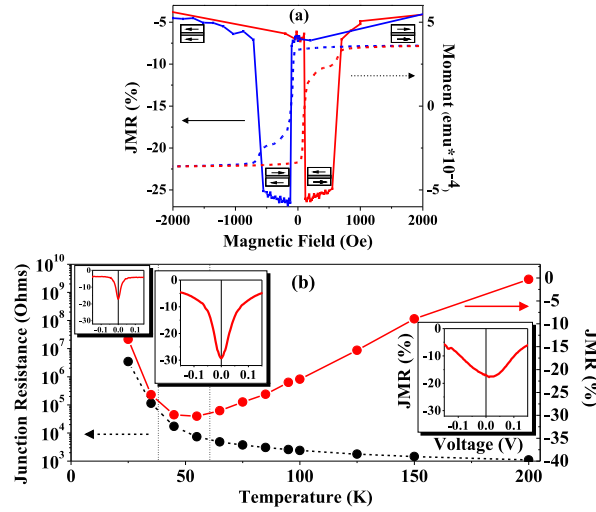


FIG. 2: (Color online) (a) Switching characteristics of $\text{Fe}_3\text{O}_4/\text{NMO}/\text{LSMO}$ junctions: magnetic hysteresis loop and resistance vs applied magnetic field at 75 K. (b) Junction resistance and maximum JMR as a function of temperature, with bias dependence of JMR for each regime.

increases in magnitude with decreasing temperature until reaching a maximum around 45 K, and then decreases with subsequent decrease in temperature. A dramatic increase in junction resistance is coincident with the decrease in JMR. A change in JMR bias dependence also occurs as a function of temperature. At high temperatures, the JMR drops off gradually at higher voltages and has a skewed, asymmetric behavior in which the JMR maximum is observed at a finite voltage. A transition occurs around 60 K, in which the bias dependence transitions to a symmetric bias dependence, characterized by a JMR maximum at zero bias, a highly symmetric shape, and a rapid decrease in JMR for $V > 50\text{-}100$ mV. At low temperatures, the bias dependence continues to be symmetric about zero bias, although the maximum JMR decreases with decreasing temperature. At these lower temperatures, the change in resistance ΔR due to the application of a magnetic field continues to increase with decreasing temperature despite the fact that the JMR decreases. Similar behavior is seen for all barrier layer thicknesses.

In order to investigate the inelastic tunneling processes in our junctions, we plot the second derivative of the IV curves, known as the IETS. The IETS illustrates the inelastic tunneling processes due to phonons and spin waves, or magnons. In order to isolate the effects of magnetism on the inelastic transport, IETS from the two distinct magnetization

configurations, $(\text{IETS})_P$ and $(\text{IETS})_{AP}$, are subtracted from one another. The resulting IETS (Fig. 3) shows inelastic tunneling events related solely to magnons as all other factors are held constant between both magnetization configurations.¹³ The $d^2I/dV^2=0$ value occurs at a finite bias for $T>60$ K, but moves towards zero bias below 60 K. The peak locations (30-50 mV) of the IETS of our junctions for all temperatures are well within the range of 12-100 mV commonly associated with magnons.^{14,15}

The observation of asymmetric bias dependence above the ordering temperature of NMO and symmetric bias dependence below the ordering temperature of NMO in both the JMR and IETS suggests that different conduction mechanisms are dominant depending on the magnetic state of the barrier. There have been numerous studies of MTJs where asymmetries in the JMR bias dependence have been attributed to two different interface density of states at the two electrode-barrier interfaces. Magnon-assisted tunneling current from electrode surface magnons has also been predicted to be asymmetric with respect to bias. Moodera *et al.* proposed that part of the large decrease in JMR with bias can be attributed to the excitation of magnons with increasing bias, which randomize the tunneling electron spins.¹⁶ Thus an asymmetry in JMR could also be caused by the unequal number of magnons created at each electrode surface as a result of the inevitable difference in the two electrode-barrier interfaces.^{13,15} In our junctions, the Fe_3O_4 -NMO interface is isostructural since both crystallize in the spinel structure; the LSMO-NMO interface is spinel/cubic perovskite where antiphase boundaries inevitably result in a more disordered interface. These two different interfaces give rise to two different barrier heights, two different interface density of states, and two different magnon density of states. Thus the asymmetry in the JMR bias dependence can be attributed to a number of mechanisms, all of which are associated with the interface.

However, while the observation of an asymmetric bias dependence due to the electrode-barrier interfaces is not unusual, the observation of a symmetric and asymmetric bias dependence of the JMR at different temperatures in the same junction is a surprising result and sheds light on the role of the barrier in the tunneling process. Such changes in symmetry are also observed in the IETS data. The asymmetric bias dependence of the IETS above the magnetic ordering temperature of the NMO is indicative of a difference in the forward and reverse magnon-assisted conduction and is consistent with transport dominated by electrode-barrier interface magnons. As the temperature is lowered below the magnetic

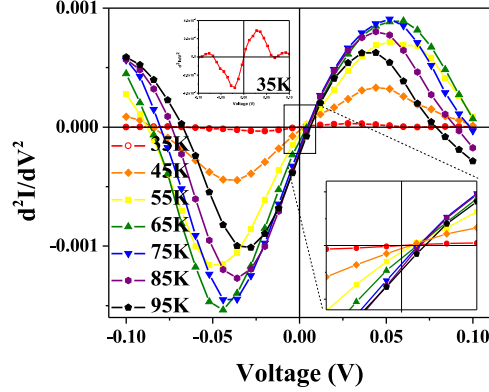


FIG. 3: (Color online) Subtracted IETS as a function of temperature, showing shift towards symmetry about zero bias below 65 K.

ordering temperature of the NMO (60 K), the bias dependence of the JMR and IETS becomes symmetric, thus suggesting that the dominant conduction mechanism is no longer sensitive to interface effects but to the bulk of the barrier. Gajek *et al.* postulated that the symmetric drop of JMR with bias for their spin filter junctions with ferromagnetic barrier layers was due to magnon excitations inside the barrier layer.¹⁷ Recalling that the subtracted IETS highlights the inelastic transport due to only magnons in the junction, the fact that the IETS becomes symmetric with respect to bias at around 60 K suggests that magnons within the barrier are beginning to influence the spin dependent transport. Such magnons from the bulk of the barrier would manifest themselves in the same way regardless of the direction of the current and thus give rise to a symmetric bias dependence both in the IETS and JMR. Furthermore, a closer look at the bias dependence of the JMR indicates a dramatic decrease in the JMR as a function of increasing bias. Below the magnon excitation energy of about 30-50 mV ascertained from the IETS data, spin polarized transport is preserved, resulting in significant JMR; above this voltage, magnons are excited and spin polarized transport is suppressed.

At even lower temperatures, the JMR bias dependence remains symmetric but the magnitude of the JMR begins to decrease around 45 K. This decrease is attributed to the dramatic increase in the junction resistance that is due to the suppressed metal-insulator transition of the Fe_3O_4 electrode, causing the electrode resistance to rival the barrier resistance.⁹ As a function of decreasing temperature, the increase in electrode resistance along with a comparable ΔR results in an overall decrease in JMR. Similar junctions with nonmagnetic barriers

also show peaks in the JMR, precluding the possibility that the decrease in the JMR is related to the magnetic transition of the barrier.⁹ The symmetric bias dependence of the JMR and the increase in ΔR in this temperature range suggests that the magnetotransport continues to be dominated by bulk magnon excitations in the NMO barrier layer.

In summary, spin polarized transport in our $\text{Fe}_3\text{O}_4/\text{NMO}/\text{LSMO}$ junctions reveals that the barrier plays an important role in the tunneling process. In these junctions, we have shown that spin transport is dominated by the interfaces or by the barrier itself depending on whether NMO is paramagnetic or ferrimagnetic. This behavior is observed via a distinct change in the bias dependence of the MTJs which coincides with the onset of ferrimagnetism in the NiMn_2O_4 barrier layer as confirmed by XMCD. When the barrier layer is paramagnetic at high temperatures, the electrode-barrier interfaces determine the asymmetric JMR bias dependence due to their different electrode-barrier surface magnon properties and different barrier heights. As the temperature is lowered, the JMR bias dependence becomes highly symmetric, suggesting a conduction mechanism involving magnons within the ferrimagnetic NMO barrier layer. Such hybrid behavior in a single junction is promising for future spintronic applications.

This work was supported in full by the Office of Basic Energy Sciences, Division of Materials Sciences and Engineering, of the U.S. Department of Energy under Contract No. DE-AC02-05CH11231. Thanks to J.S. Moodera for fruitful discussion. Processing was performed in the University of California - Berkeley Microlab.

* Electronic address: bbnelsonchee@berkeley.edu

¹ M. Julliere, *Phys. Lett.* **54A**, 225 (1975).

² J.S. Moodera, L.R. Kinder, T.M. Wong, and R. Meservey, *Phys. Rev. Lett.* **74**, 3273 (1995).

³ G.T. Woods, R.J. Soulen, Jr., I.I. Mazin, B. Nadgorny, M.S. Osofsky, J. Sanders, H. Srikanth, W.F. Egelhoff, and R. Datla, *Phys. Rev. B.* **70**, 054416 (2004).

⁴ W.H. Butler, X.-G. Zhang, T.C. Schulthess, and J.M. MacLaren, *Phys. Rev. B* **63**, 054416 (2001).

⁵ R. Jansen, and J.S. Moodera, *Appl. Phys. Lett.* **75**, 400 (1999).

⁶ R. Jansen, and J.C. Lodder, *Phys. Rev. B* **61**, 5860 (2000).

- ⁷ M-H. Jo, N.D. Mathur, N.K. Todd, and M.G. Blamire, Phys. Rev. B **61**, R14905 (2000).
- ⁸ G. Hu, and Y. Suzuki, Phys. Rev. Lett. **89**, 276601 (2002), and references therein.
- ⁹ L.M.B. Alldredge, R.V. Chopdekar, B. Nelson-Cheeseman, and Y. Suzuki, Appl. Phys. Lett. **89**, 182504 (2006).
- ¹⁰ B.B. Nelson-Cheeseman, R.V. Chopdekar, M.F. Toney, J.S. Bettinger, E. Arenholz, and Y. Suzuki. (Unpublished).
- ¹¹ R. Stadler, Y.U. Idzerda, Z. Chen, S.B. Ogale, and T. Venkatesan, Appl. Phys. Lett. **75**, 3384 (1999).
- ¹² B.B. Nelson-Cheeseman, R.V. Chopdekar, J.S. Bettinger, E. Arenholz, and Y.Suzuki. [arXiv:0709.3518](https://arxiv.org/abs/0709.3518) [cond-mat.str-el]
- ¹³ J.S. Moodera, J. Nowak, and R.J.M. van de Veerdonk, Phys. Rev. Lett. **80**, 2941 (1998).
- ¹⁴ D.C. Tsui, R.E. Dietz, and L.R. Walker, Phys. Rev. Lett. **27**, 1729 (1971).
- ¹⁵ Y. Ando, J. Murai, H. Kubota, and T. Miyazaki, J. Appl. Phys. **87**, 5209 (2000).
- ¹⁶ J.S. Moodera, and G. Mathon, J. Magn. Magn. Mater. **200**, 248 (1999).
- ¹⁷ M. Gajek, M. Bibes, A. Barthelemy, K. Bouzehouane, S. Fusil, M. Varela, J. Fontcuberta, and A. Fert, Phys. Rev. B **72**, 020406(R) (2005).